Comparative μ^+SR investigation of static magnetic order and anisotropy of the pure and Pb-doped $Bi_2Sr_2Co_2O_y$ layered cobalt dioxides

Jun Sugiyama,[1,*] Yutaka Ikedo,[1] Hiroshi Nozaki,[1] Peter L. Russo,[2] Jess H. Brewer,[3] Eduardo J. Ansaldo,[2] Gerald D. Morris,[2] Kim H. Chow,[4] Scott L. Stubbs,[5] Daniel Andreica,[6] Alex Amato,[7] Takenori Fujii,[8] Satoshi Okada,[9] and Ichiro Terasaki[9]

[1]*Toyota Central Research and Development Laboratories Inc., Nagakute, Aichi 480-1192, Japan*

[2]*TRIUMF, 4004 Wesbrook Mall, Vancouver, BC, V6T 2A3, Canada*

[3]*TRIUMF, CIfAR and Department of Physics and Astronomy, University of British Columbia, Vancouver, BC, V6T 1Z1, Canada*

[4]*Department of Physics, University of Alberta, Edmonton, AB, T6G 2G7, Canada*

[5]*Department of Physics and Astronomy, University of British Columbia, Vancouver, BC, V6T 1Z1, Canada*

[6]*Faculty of Physics, Babes-Bolyai University, 3400 Cluj-Napoca, Romania*

[7]*Laboratory for Muon-Spin Spectroscopy, Paul Scherrer Institut, CH-5232 Villigen PSI, Switzerland*

[8]*Cryogenic Center, University of Tokyo, 2-11-16 Yayoi, Bunkyo-ku, Tokyo 113-0032, Japan*

[9]*Department of Applied Physics, Waseda University, Tokyo 169-8555, Japan*

(Received 16 April 2008; revised manuscript received 4 August 2008; published 25 September 2008)

The magnetism of pure and Pb-doped $Bi_2Sr_2Co_2O_y$ (BSCO) crystals has been investigated with positive muon-spin rotation and relaxation (μ^+SR) spectroscopy. The entire volume of both materials enters into a magnetic state at low temperatures, occurring below 4.7 K for Pb-doped BSCO and below 1.0 K for pristine BSCO. By combining μ^+SR and susceptibility measurements, it is clarified that Pb-doped BSCO is a ferromagnet with a Curie temperature (T_C) of 4.7 K and its ordered internal magnetic field ($H_{\rm int}$) is almost parallel to the c axis. Since the relationship between the reduced T and reduced $H_{\rm int}$ for Pb-doped BSCO is very similar to that for BSCO, the origin of the magnetic transition in both crystals is thought to be explained by common physics. Interestingly, we also detect the existence of a magnetic anomaly far above T_C. This occurs at $\approx$60 K, coinciding with the metal-to-insulator transition that was observed for both materials by resistivity measurements.

DOI: 10.1103/PhysRevB.78.094422 PACS number(s): 76.75.+i, 75.30.Kz, 75.50.Ee

I. INTRODUCTION

Layered cobalt dioxides with a triple or a quadruple rock-salt (RS)-type block, such as $[A_2BO_3]_z^{RS}[CoO_2]$ and $[A_2B_2O_4]_z^{RS}[CoO_2]$, where A is an alkali earth ion (Ca, Sr, and Ba) and B is Tl, Bi, Pb, Co, and Cu,[1–4] exhibit complex successive magnetic transitions.[5–7] These transitions are believed to be a consequence of two types of interactions. The first of these is the intraplane interaction between Co moments in the same CoO_2 plane. The other interaction is the interplane interaction between adjacent CoO_2 planes, mediated through magnetic ions in the RS-type block. It is therefore interesting to investigate how the magnetic nature of the layered cobalt dioxides will be modified if the interplane interaction is absent, such as in the system $[Bi_2Sr_2O_4]_{\sim 0.5}^{RS}[CoO_2]$ (BSCO), in which there are no magnetic ions in the RS-type block.

The T dependence of the in-plane resistivity (ρ) for BSCO crystals, particularly the resistivity along the b axis, (ρ_b) is known to decrease in proportion to T down to $\sim$50 K (metallic behavior) and then increase with increasing slope upon further cooling (insulating behavior).[8,9] It is thus proposed that the energy gap (pseudo gap), presumably due to the formation of antiferromagnetic (AF) order at $\sim$60 K, plays a significant role in determining the transport properties of BSCO.[9] However, recent μ^+SR experiments on BSCO and the related compound $[Ba_2Bi_{1.8}Co_{0.2}O_4]_{0.5}^{RS}[CoO_2]$ indicated the absence of either long-range or short-range magnetic orders down to 2 K.[10] The origin of the metal-to-insulator transition around 60 K is thus still an open question.

Interestingly, the temperature at which the $\rho_b(T)$ curve shows a minimum ($T_{\rm min}$) slightly depends on the Pb concentration x in $[Bi_{2-x}Pb_xSr_2O_4]_{\sim 0.5}^{RS}[CoO_2]$ (Pb_x–BSCO).[11] The highest $T_{\rm min}$ (=60 K) was observed for $Pb_{0.4}$–BSCO.[9] Note also that the substitution of Bi^{3+} by Pb^{2+} reduces the magnitude of ρ systematically in the x range up to 0.6, reflecting the increased doping of carriers into the CoO_2 planes.[8,9,11] Such doping, naturally and drastically, alters the physical properties of Pb_x–BSCO. This is analogous to the situation observed in Na_xCoO_2, which exhibits a complex electronic/magnetic phase diagram as a function of x.[12] According to magnetic-susceptibility (χ) measurements on Pb_x–BSCO,[8] the Pb doping increases the ferromagnetic (FM) interaction between Co moments. This is evidenced by the dependence of the Weiss temperature, varying from Θ_p=−2.1 K for Pb_0–BSCO to 9.9 K for $Pb_{0.2}$–BSCO and to 18.8 K for $Pb_{0.4}$–BSCO. Furthermore, a spin-glass like transition was found for $Pb_{0.44}$–BSCO at $T_f\sim$3 K and long-range magnetic order for $Pb_{0.51}$–BSCO below T_C=4.5 K,[8] although the magnetic structure is not fully understood. A systematic investigation of the microscopic magnetic nature of Pb_x–BSCO is therefore necessary to clarify the mechanism of the minimum in the $\rho(T)$ curve and the magnetism below T_f or T_C.

Among the various magnetic measurement techniques, μ^+SR is particularly sensitive to the local magnetic environment[13] because the μ^+ interacts with predominantly its nearest neighbors. It is therefore also sensitive to short-range magnetic order, which sometimes appears in low-dimensional systems, while both neutron-scattering and χ

measurements mainly detect long-range magnetic order. Also, zero-field (ZF)-μ^+SR, i.e., μ^+SR measurements carried out in the absence of an applied field, is uniquely sensitive to weak local magnetic [dis]order produced by quasistatic electronic spins.

In this paper, we report mainly on ZF-μ^+SR studies obtained on a single crystal of $Pb_{0.4}$−BSCO ($Bi_{1.6}Pb_{0.4}Sr_2Co_2O_y$) measured at temperatures between 1.8 and 200 K. We clearly demonstrate that $Pb_{0.4}$−BSCO is entirely paramagnetic above 5 K, but the whole sample volume exhibits a ferromagnetically ordered state below ~5 K. We also report the μ^+SR results on a pure single crystal of BSCO, which was previously believed to be a paramagnet down to the lowest T measured. We find instead that BSCO undergoes a magnetic transition at 1.0 K, probably into a ferromagnetic state analogous to the one observed in $Pb_{0.4}$−BSCO. Finally, we describe weak longitudinal field (wLF)-μ^+SR measurements on both $Pb_{0.4}$−BSCO and BSCO, which show a small change in the local magnetism at ~60 K.

II. EXPERIMENT

A single crystal of $Pb_{0.4}$−BSCO was grown at Waseda University by a traveling solvent floating zone technique. The dimension of a crystal ingot was about 5 and 80 mm in diameter and length, respectively. The ingot was cut and cleaved to make a sample plate with about $5\times5\times0.5$ mm^3. The preparation and characterization of the sample were reported in greater detail elsewhere.[9] The μ^+SR spectra were measured at the M15 and M20 surface muon beam lines at TRIUMF (Canada) and the πM3.2-GPS and πE1-Dolly surface muon beam lines at PSI (Switzerland). Four crystals were arrayed in an active-muon-veto sample holder with their c axes parallel to the beam direction and their growth direction parallel to the vertical direction (and perpendicular to the beam direction). Since the angle between the growth direction and a axis was either ~50° or ~75°, the c plane was found to consist of mainly two domains. In other words, although we used the single crystals, the obtained signal in the c plane was the average of the signals along the a and b axes. Muon-spin rotation and relaxation spectra were obtained mainly in zero applied field with four positron detectors [backward (B), forward (F), up (U), and down (D)]. The initial direction of the muon polarization [$\boldsymbol{S}_\mu(0)$] relative to the c plane of the crystals was set by a Wien filter spin rotator. The experimental setup (see Fig. 1) and procedures are described in more detail elsewhere.[13]

Susceptibility (χ) was measured using a superconducting quantum interference device magnetometer (MPMS, Quantum Design) in the T range between 400 and 5 K under magnetic field $\boldsymbol{H}\leq100$ Oe. In order to determine anisotropy, H was applied parallel or perpendicular to the c plane. Hereby, we will abbreviate susceptibility obtained with $\boldsymbol{H}\|\boldsymbol{c}$ as χ_c and $\boldsymbol{H}\perp\boldsymbol{c}$ as χ_{ab}, respectively. Heat capacity (C_p) was measured using a relaxation technique (PPMS, Quantum Design) in the T range between 300 and 1.9 K.

III. RESULTS

A. Result for $x=0.4$

In order to demonstrate the magnetic transition at low T, Fig. 2 shows the weak transverse field (wTF) spectra at 6, 5, 4, and 3 K obtained with wTF=30 Oe on $Pb_{0.4}$−BSCO. Here, "weak" means relative to possible spontaneous internal fields ($H_{\rm int}$) in the ordered state. A wTF-μ^+SR technique is sensitive to local magnetic order via the shift of the μ^+ spin precession frequency and the enhanced μ^+ spin relaxation. As T decreases from 6 K, the oscillation amplitude due to wTF rapidly decreases, indicating the appearance of a spontaneous internal field $H_{\rm int}$. The wTF-μ^+SR spectra were therefore fitted using a combination of a slowly relaxing precessing signal and a fast relaxing nonoscillatory signal. The first component is due to wTF and the latter due to $H_{\rm int}$,

$$A_0P_{\rm TF}(t)=A_{\rm TF}\cos(\omega_{\rm TF}^{\mu}t+\phi_{\rm TF})\exp\left(-\frac{\sigma_{\rm TF}^2t^2}{2}\right)+A_{\rm fast}\exp(-\lambda_{\rm fast}t), \quad (1)$$

where A_0 is the initial ($t=0$) asymmetry, $P_{\rm TF}(t)$ is the muon-spin polarization function, $\omega_{\rm TF}^{\mu}$ is the muon Larmor frequency corresponding to the applied wTF, $\phi_{\rm TF}$ is the initial phase of the precessing signal, $\sigma_{\rm TF}$ is the Gaussian relaxation rate of the precessing signal, $\lambda_{\rm fast}$ is the exponential relaxation rate of the nonoscillatory signal, and $A_{\rm TF}$ and $A_{\rm fast}$ are

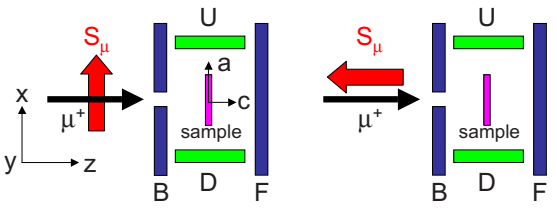

FIG. 1. (Color online) Geometry of the μ^+SR experiment: four counters [backward (B), forward (F), up (U), and down (D)] detect decay positrons emitted in the $-z$, $+z$, $+x$, and $-x$ directions, respectively. The initial muon-spin direction $\boldsymbol{S}_\mu(0)$ is in the $+x$ direction ($\perp\boldsymbol{c}$ of the crystals) for spin-rotated (SR) mode (a) or in the $-z$ direction ($\|\boldsymbol{c}$) for nonspin-rotated (NSR) mode (b). Thus if the internal magnetic field ($\boldsymbol{H}_{\rm int}$) is parallel to $\boldsymbol{c}$, only U and D counters will detect a muon-spin oscillation, and that only in SR mode; but if $\boldsymbol{H}_{\rm int}\perp\boldsymbol{c}$, only B and F counters in NSR mode will show an oscillatory signal.

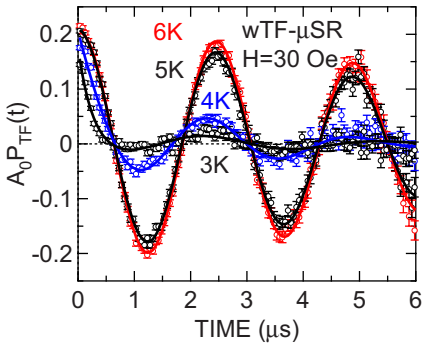

FIG. 2. (Color online) Variation of the wTF-μ^+SR time spectra with T for the $Bi_{1.6}Pb_{0.4}Sr_2Co_2O_y$ crystal. The configuration of the sample and $\boldsymbol{S}_\mu(0)$ is $\boldsymbol{S}_\mu(0)\|\boldsymbol{c}$. The solid lines show the fitting results using Eq. (1).

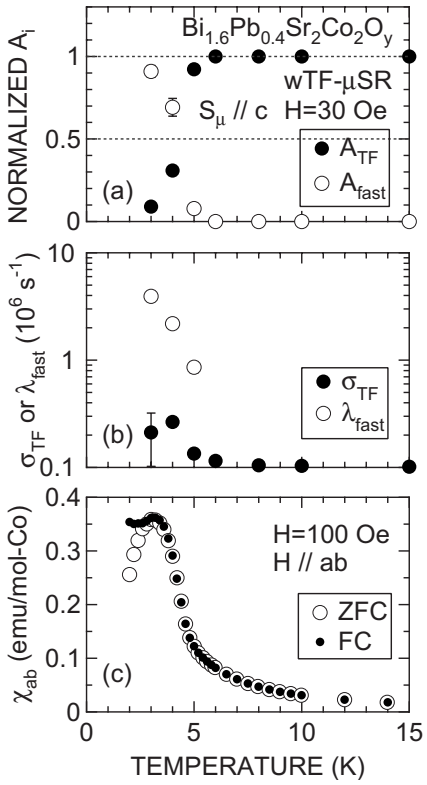

FIG. 3. Temperature dependences of (a) normalized asymmetries (A_{TF} and A_{fast}), (b) relaxation rates (σ_{TF} and λ_{fast}), and (c) susceptibility in the *ab* plane (χ_{ab}) for the $Bi_{1.6}Pb_{0.4}Sr_2Co_2O_y$ crystal. The data were obtained by fitting the wTF spectrum using Eq. (1). χ was measured in both zero-field-cooling (ZFC) and field-cooling (FC) modes with $H=100$ Oe.

the asymmetries of the two components of the μ^+SR signal.

Figure 3 shows the T dependences of [Fig. 3(a)] normalized asymmetries ($N_{A_i}=A_i/A_0$ with i=TF and fast), [Fig. 3(b)] relaxation rates (σ_{TF} and λ_{fast}), and [Fig. 3(c)] χ. Upon decreasing T below 6 K, $N_{A_{\mathrm{TF}}}$, which corresponds to the volume fraction V_F of paramagnetic (PM) phases in a sample, shows a clear drop and reaches almost zero at 3 K. This drop points to the occurrence of a bulk magnetic transition at ~4.5 K, at which $N_{A_{\mathrm{TF}}}=0.5$. The relaxation of the fast component $\lambda_{\mathrm{fast}}(T)$ shows a sudden increase below 5 K accompanying the decrease (increase) observed in $N_{A_{\mathrm{TF}}}$ ($N_{A_{\mathrm{fast}}}$). The observation of a bulk transition at ~4.5 K is fully consistent with the $\chi(T)$ curve shown in the lower panel of Fig. 3.

In order to elucidate the microscopic magnetic nature of $Pb_{0.4}$−BSCO, particularly below 4.5 K, ZF-μ^+SR spectra were also recorded. Figure 4(a) shows ZF-μ^+SR time spectra recorded at 1.8 K. A clear first minimum is observed for the different geometrical configurations. However, the difference between both spectra points to an anisotropic magnetic structure for $Pb_{0.4}$−BSCO. Although the overall time spectrum is satisfactorily reproduced by a Kubo-Toyabe (KT) function (representing the muon-spin relaxation due to randomly oriented magnetic moments), we need an additional fast relaxed nonoscillatory signal for explaining the rapid decay in the early time domain (below 0.15 μs) of the ZF spectrum, particularly for the spectrum obtained with the $\boldsymbol{S}_\mu(0)\perp\boldsymbol{c}$ configuration. Furthermore, in order to check the KT behavior, we measured longitudinal-field (LF) spectra as the change in the KT signal with LF is well modeled by considering the alignment of the random moments along the direction of the applied LF. As shown in Fig. 4(b), the LF dependence of the spectra is not well fitted by a static/dynamic Gaussian KT function. Actually, the anisotropic behavior in Fig. 4(a) naturally excludes the possibility of the KT behavior for $Pb_{0.4}$−BSCO, when both spectra obtained with the $\boldsymbol{S}_\mu(0)\perp\boldsymbol{c}$ and $\boldsymbol{S}_\mu(0)\|\boldsymbol{c}$ are not fitted only by the KT signal.[14] We thus use a combination of an exponentially damped cosine oscillation signal and a slow exponential relaxing nonoscillatory signal for fit the ZF spectrum,

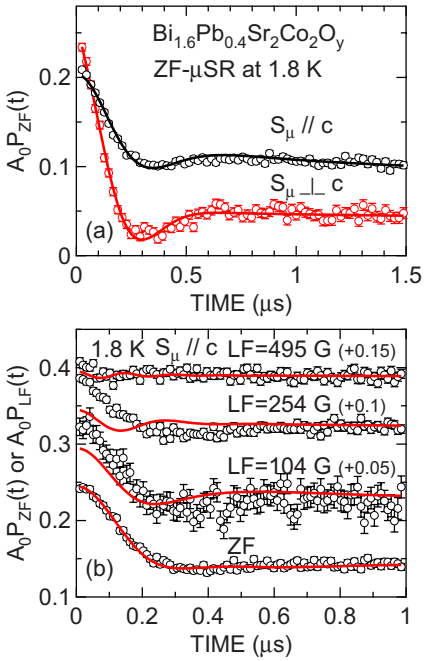

FIG. 4. (Color online) (a) ZF-μ^+SR time spectra obtained on $Bi_{1.6}Pb_{0.4}Sr_2Co_2O_y$ at 1.8 K. Measurements were performed with $\boldsymbol{S}_\mu(0)\|\boldsymbol{c}$ and $\boldsymbol{S}_\mu(0)\perp\boldsymbol{c}$. (b) ZF and longitudinal-field (LF) μ^+SR time spectra at 1.8 K obtained with the configurations $\boldsymbol{S}_\mu(0)\|\boldsymbol{c}$. The solid lines of (a) show the fitting results using Eq. (2) and those of (b) using a dynamic Gaussian Kubo-Toyabe function.

$$A_0P_{\mathrm{ZF}}(t)=A_M\exp(-\lambda_M t)\cos(\omega_M^\mu t+\phi)+A_{\mathrm{tail}}\exp(-\lambda_{\mathrm{tail}}t), \tag{2}$$

where A_M and A_{tail} are the asymmetries of the two signals, λ_M and λ_{tail} are their relaxation rates, ω_M^μ is the muon precession frequency due to H_{int} ($\omega_M^\mu/2\pi=13.554$ kHz/Oe $\times H_{\mathrm{int}}$), and ϕ is the initial phase of the precession. The fitted values of ϕ are less than 6°, i.e., close to 0°, suggesting commensurate magnetic order below T_M. Note that the additional tail component is small (below 0.05) and it probably arises from a small deviation of the angle from 0 or 90° between $\boldsymbol{S}_\mu(0)$ and the crystallographic axis. It is therefore concluded that $Pb_{0.4}$−BSCO is in a magnetically ordered state below ~4.5 K ($=T_M$).

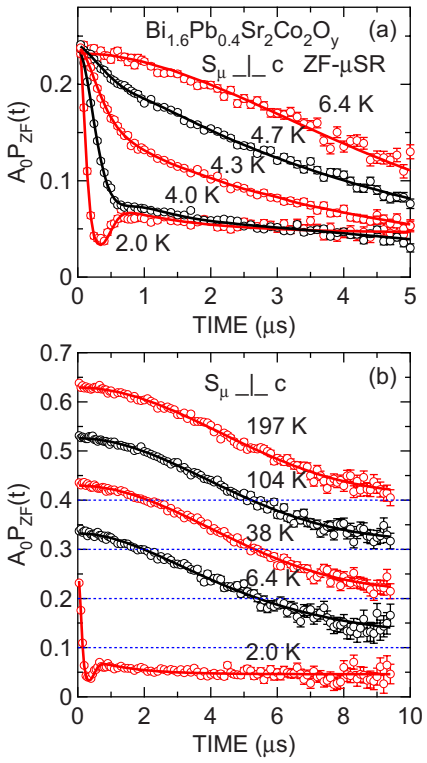

FIG. 5. (Color online) Temperature dependence of ZF-μ^+SR spectrum for the $Bi_{1.6}Pb_{0.4}Sr_2Co_2O_y$ crystal; (a) below 6.4 K and (b) between 2.0 and 197 K. The configuration of the sample and the initial muon-spin direction ($\boldsymbol{S}_\mu(0)$) is $\boldsymbol{S}_\mu(0) \perp \boldsymbol{c}$. In (b), each spectrum is offset by 0.1 for clarity of the display. The solid lines show the fitting results using Eqs. (2) and (3).

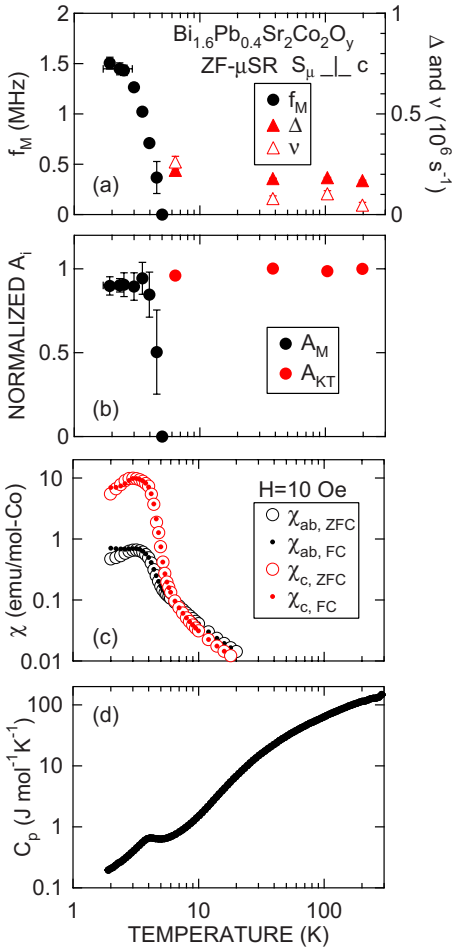

FIG. 6. (Color online) Temperature dependences of (a) f_M ($\equiv \omega_M^\mu/2\pi$), Δ, and ν, (b) normalized A_M and A_{KT}, (c) χ_{ab} and χ_c, and (d) heat capacity (C_p) for $Bi_{1.6}Pb_{0.4}Sr_2Co_2O_y$. The μ^+SR data were obtained by fitting the ZF-μ^+SR spectrum measured with the $\boldsymbol{S}_\mu(0) \perp \boldsymbol{c}$ configuration using Eq. (2) below 6.4 K and Eq. (3) above 6.4 K.

Figure 5 shows the T dependence of the ZF-μ^+SR spectra in the T range between 2.0 and 197 K. As T increases from 2 K, the signature of the damped cosine signal—i.e., the first minimum, disappears at around 4 K and then the exponential relaxation rate decreases with further increasing T. At 6.4 K, the whole spectrum exhibits a slow Gaussian-type relaxation and it is found that the ZF spectrum is almost T independent above 6.4 K. Above this temperature, the relaxation of the ZF spectra is therefore solely due to randomly oriented nuclear magnetic moments,[13] i.e., ^{209}Bi, ^{207}Pb, ^{87}Sr, and (mainly) ^{59}Co. The ZF spectrum at $T \geq 6.7$ K was therefore fitted only by a dynamic Gaussian KT function,

$$A_0 P_{ZF}(t) = A_{KT} G^{DGKT}(t, \Delta, \nu), \tag{3}$$

where Δ is the static width of the local frequencies at the disordered sites and ν is the field fluctuation rate. When $\nu = 0$, $G^{DGKT}(t, \Delta, \nu)$ is the static Gaussian KT function $G_{zz}^{KT}(t, \Delta)$ given by

$$G_{zz}^{KT}(t, \Delta) = \frac{1}{3} + \frac{2}{3}(1 - \Delta^2 t^2)\exp\left(-\frac{\Delta^2 t^2}{2}\right). \tag{4}$$

The ZF spectra in the whole T range measured were therefore fitted by Eq. (2) at $T \leq 5$ K and by Eq. (3) at $T \geq 6.4$ K. Figure 6 shows the T dependences of [Fig. 6(a)] $f_M(\equiv \omega_M^\mu/2\pi)$, Δ, and ν; [Fig. 6(b)] normalized A_M and A_{KT}; [Fig. 6(c)] χ_{ab} and χ_c; and [Fig. 6(d)] heat capacity (C_p) for $Pb_{0.4}$−BSCO. Below 4.5 K, f_M is nonzero and as T decreases from 4.5 K, f_M increases with decreasing slope (df_M/dT). The value of f_M seems to level off to its maximum value ($\sim$1.5 MHz) below around 3 K. Such behavior is reasonable for the order parameter of the magnetic transition. Since $N_{A_M} \sim 1$ at 2 K, the whole sample is in the magnetically ordered state as found by the wTF measurements. As T increases from 2 K, the volume of the A_M component decreases with T, with a particularly sharp drop in the vicinity of T_M, and finally disappears above T_M. The A_{KT} component appears above T_M and the volume fraction of the KT signal due to the PM phase reaches almost 100% by 6.4 K, suggesting a sharp transition from a low-T ordered phase to a high-T PM phase at T_M.

As seen in Fig. 6(a), the magnitude of Δ is almost T independent above T_M. Also, although $\nu \sim \Delta$ at 6.4 K, ν decreases with increasing T and reaches almost 1/10 of Δ at 197 K, indicating a static nature of the KT signal in the PM phase as expected. Only in the vicinity above T_M, both Δ and ν have large values compared with that above 6.4 K. We wish here to emphasize again the lack of the indication of a

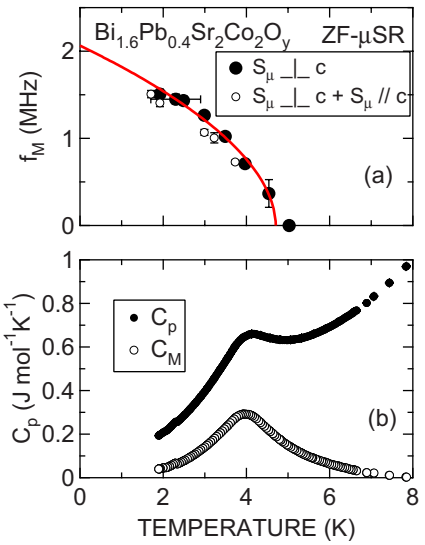

FIG. 7. (Color online) Temperature dependences of (a) f_M and (b) C_p and C_M for $Bi_{1.6}Pb_{0.4}Sr_2Co_2O_y$. Solid circles in (a) represent the data obtained by fitting only the ZF spectrum with $\boldsymbol{S}_\mu(0) \perp \boldsymbol{c}$ configuration [same to those in Fig. 6(a)], while open circles show the data obtained by fitting the two ZF spectra with $\boldsymbol{S}_\mu(0) \perp \boldsymbol{c}$ and $\boldsymbol{S}_\mu(0) \| \boldsymbol{c}$ configuration simultaneously. The solid lines in (a) show the fitting result using the formula $f_M/f_M(0\ \mathrm{K}) = (1 - T/T_M)^\beta$. C_M was obtained by the formula $C_p = C_M + C_L$, where C_L is the lattice specific heat and is estimated from the linear relationship between C_p/T and T^2 in the T^2 range between 60 and 300 K^2.

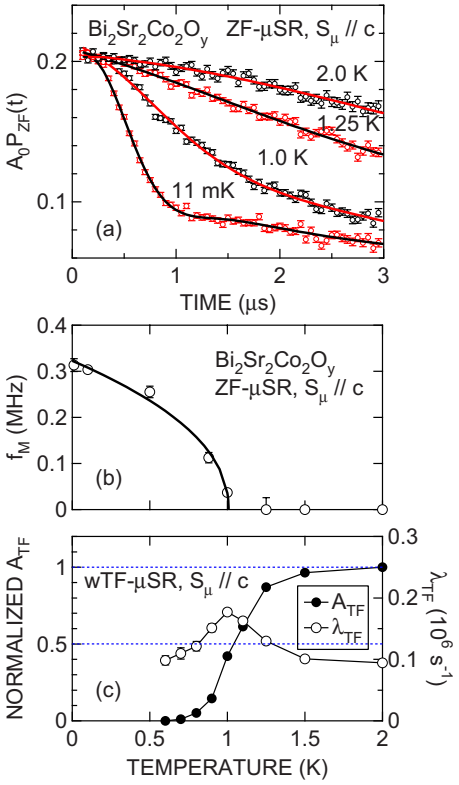

FIG. 8. (Color online) Temperature dependences of (a) ZF-μ^+SR spectrum, (b) f_M, and (c) normalized asymmetries (A_TF) and relaxation rates (σ_TF) for the $Bi_2Sr_2Co_2O_y$ crystal. The configuration is $\boldsymbol{S}_\mu(0) \| \boldsymbol{c}$. The solid lines in (a) show the fitting results using Eq. (2) and that in (b) represents the fitting using the formula $f_M/f_M(0\ \mathrm{K}) = (1 - T/T_M)^\beta$. The wTF data were obtained by fitting the wTF spectrum measured with the $\boldsymbol{S}_\mu(0) \| \boldsymbol{c}$ configuration using Eq. (1).

magnetic transition above T_M because $N_{A_\mathrm{KT}} \sim 1$ in the whole T range above T_M. The T-independent Δ above T_M also supports this conclusion.

In order to elucidate the variation of the internal magnetic field (H_int) with T below the vicinity of T_M, Fig. 7 shows f_M as a function of T together with the magnetic heat capacity (C_M). The $f_M(T)$ curve exhibits a monotonic increase with decreasing T. If we employ a general relation $f_M/f_M(0\ \mathrm{K}) = [1 - (T/T_M)]^\beta$, we obtain $f_M(0\ \mathrm{K}) = 2.06 \pm 0.11$ MHz, $T_M = 4.7 \pm 0.1$ K, and $\beta = 0.53 \pm 0.08$, respectively. While the reasons are currently unknown, the value of β is significantly higher than β for the related compounds that shows the transition to the AF ordered phase. That is, $\beta = 0.28$ for $Na_{0.75}CoO_2$ (Ref. 15) and $\beta = 0.24$ for $NaNiO_2$.[16] Note that T_M, determined by the $f_M(T)$ curve, ($T_M^{\mu\mathrm{SR}}$) is higher by 0.7 K than that by the $C_M(T)$ curve ($T_M^{C_P} = 4$ K), but is in good agreement with T_M determined by the $\chi_\mathrm{ab}(T)$ curve, which increases rapidly with decreasing T below ~ 5 K ($= T_M^\chi$). The overall T_M is therefore determined as 4.7 K for $Pb_{0.4}$–BSCO. The discrepancy between $T_M^{C_P}$ and $T_M^{\mu\mathrm{SR}}$ highlights the characteristic feature of μ^+SR, which is very sensitive to a local magnetic order/disorder. Finally, the relatively wide peak in the $C_M(T)$ curve at $T_M^{C_P}$ is consistent with the shape of the ZF spectrum of $Pb_{0.4}$–BSCO, in particular, only the first minimum is observable even at the lowest temperature studied, i.e., 1.8 K, suggesting a wide field distribution in the ordered state. However, the fact that $T_M^{C_P} < T_M^{\mu\mathrm{SR}}(T_M^\chi)$ rules out the possibility of a spin-glass transition at T_M.[17]

B. Comparison with $x = 0$

Although previous work on the pure sample BSCO showed the absence of magnetic transitions down to 1.8 K,[10] many other layered cobalt dioxides are known to exhibit a magnetic transition at low T due to the order of Co moments in the CoO_2 plane. We thus measured the wTF- and ZF-μ^+SR spectra for the BSCO single crystals down to 11 mK using a dilution refrigerator (DR). Figure 8(a) shows the ZF spectra with the $\boldsymbol{S}_\mu(0) \| \boldsymbol{c}$ configuration for BSCO in the T range between 1.5 K and 11 mK. In spite of a large background signal even at 11 mK, i.e., a slowly exponential relaxation signal from the muons stopped outside the sample (mainly in the silver holder and inside of the DR), the spectrum at 11 mK exhibits a first broad minimum at around 1 μs. This suggests the existence of a static order with wide field distribution as well as for $Pb_{0.4}$–BSCO. As T increases from 11 mK, the minimum shifts toward a longer time and then the spectrum shows a typical KT behavior above 1.25 K. The change of the ZF spectrum with T is very similar to that of $Pb_{0.4}$–BSCO [see Fig. 5(a)] if we ignore the difference of the time at which the spectrum shows a minimum.

Actually, as seen in Fig. 8(b), the $f_M(T)$ curve is also well fitted by the formula $f_M/f_M(0\ \mathrm{K}) = (1 - T/T_M)^\beta$ with $f_M(0\ \mathrm{K}) = 0.329 \pm 0.02$ MHz, $T_M = 1.01 \pm 0.02$ K, and β

$=0.48\pm0.12$ in the whole T range below T_M. The $N_{A_{TF}}(T)$ curve also demonstrates the existence of a bulk magnetic transition at ~1 K for BSCO [see Fig. 8(c)]. Therefore, β of BSCO is reasonably consistent with β of $Pb_{0.4}$–BSCO (0.53 ± 0.08) within the estimated error [see Fig. 7(a)]. This also suggests that, although $f_M(0\ \mathrm{K})$ (T_M) for BSCO is ~1/7 (~1/5) of that for $Pb_{0.4}$–BSCO, the origin of the transition of BSCO is essentially the same to that of $Pb_{0.4}$–BSCO. In other words, the magnitude of T_M is found to strongly depend on the spin concentration in the CoO_2 plane, as in the case for the other layered cobalt dioxides. Since Fig. 6(d) clearly supports the appearance of FM order below $T_M(\equiv T_C)$ for $Pb_{0.4}$–BSCO, BSCO is also most likely to enter into the FM phase below T_M. The magnetic structure of $Pb_{0.4}$–BSCO and BSCO will be discussed in Sec. IV.

C. Resistivity minimum at ~60 K for $x=0$ and 0.4

As can be seen in Figs. 5 and 8(a), the ZF spectrum exhibits only a slow relaxation due to nuclear moments above T_M, indicating a PM regime for $Pb_{0.4}$–BSCO and BSCO. However, if the change in the μ^+SR parameters accompanying the formation of magnetic order is very small due to low dimensionality and/or geometrical frustration, the anomaly would be hidden by the relaxation due to nuclear moments, mainly, ^{59}Co. We thus measured the wLF spectrum, with wLF=30 Oe, to decouple the nuclear moments.

Figure 9(a) shows the T dependence of the exponential relaxation rate for both $Pb_{0.4}$–BSCO and BSCO. It is found that $\lambda_{LF}(T)$ curve exhibits a local maximum at ~60 K $(=T_A)$ for both crystals, around which the $\rho(T)$ curves show the broad minimum $(=T_{min})$ [see Figs. 9(b) and 9(c)]. Although the magnetic transition occurs at $T_M\sim5$ K (~1 K) for $Pb_{0.4}$–BSCO (BSCO) as described above, the energy scale of T_M is 10–50 times smaller than that of T_A. It is therefore difficult to consider that the origin of T_A is a precursory phenomenon of T_M. The increase in λ_{LF} below T_A implies that the distribution of an internal magnetic field becomes inhomogeneous with decreasing T. While the origin of such inhomogeneous field distribution is currently unknown, the following scenarios are possible: formation of a very short-range SDW, local charge order accompanying a small structural variation, appearance of magnetic clusters, and/or a partial spin-state transition of Co ions. In conclusion, the wLF result suggests that the microscopic magnetic environment at the μ^+'s changes slightly around 60 K. In order to further elucidate its origin, a precise structural analysis as a function of T and/or neutron inelastic-scattering experiments are needed using a high-quality single-crystal sample. In addition, a similar situation may apply for other layered cobalt dioxides with quadruple RS-type block $[Bi_2M_2O_4]_x^{RS}[CoO_2]$ (M=Ba, Sr, and Ca),[18] in which only wTF measurements were done, but such effects are seen only by the wLF measurements.

IV. DISCUSSION

A. Anisotropic feature

In order to evaluate the magnetic anisotropy shown in Fig. 4(a), the two ZF spectra were fitted simultaneously using Eq.

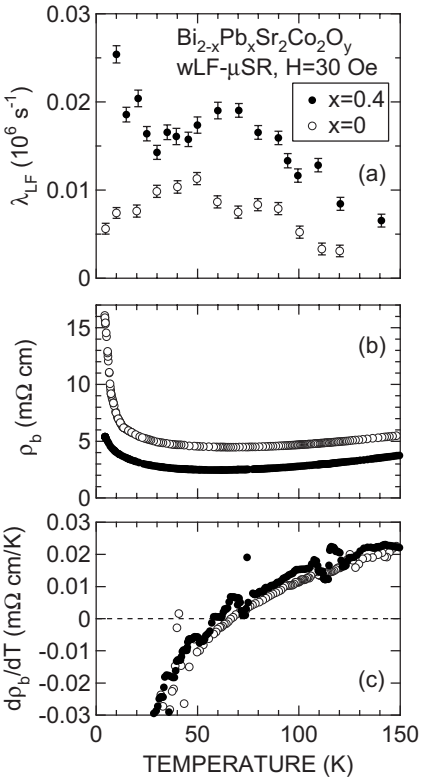

FIG. 9. Temperature dependence of (a) weak longitudinal-field- (wLF) relaxation rate (λ_{LF}) and (b) resistivity (ρ_b) (Ref. 9), and (c) its slope ($d\rho_b/dT$) for $Bi_{1.6}Pb_{0.4}Sr_2Co_2O_y$ and $Bi_2Sr_2Co_2O_y$. The wLF data were obtained by fitting the wLF-μ^+SR spectrum observed with the $\boldsymbol{S}_\mu(0)\|\boldsymbol{c}$ configuration using an exponential relaxation function $A_{LF}\exp(-\lambda_{LF}t)$.

(2). The fit provides that $A_{M,c}^{\perp c}=0.201\pm0.003$ and $A_{M,ab}^{\|c}=0.099\pm0.003$, respectively. Here, $A_{M,c}^{\perp c}$ means the amplitude of oscillation along the c axis detected in the configuration with $S_\mu(0)\perp\boldsymbol{c}$, while $A_{M,ab}^{\|c}$ is the amplitude of oscillation in the c plane, which is detected in the configuration with $S_\mu(0)\|\boldsymbol{c}$. The angle of A_M component to the c plane (θ) is simply estimated as $\theta_M^{\perp c\|c}=\tan^{-1}(A_{M,c}^{\perp c}/A_{M,ab}^{\|c})=\tan^{-1}(0.201/0.099)=64\pm1°$. The same fit also provides $\theta_M^{\perp c\perp c}=\tan^{-1}(A_{M,c}^{\perp c}/A_{M,ab}^{\perp c})=\tan^{-1}(0.201/0.041)=78.5\pm0.7°$. Note that $\boldsymbol{S}_\mu(0)$ is slightly rotated by ~10° to avoid direct positrons from the muon target when $\boldsymbol{S}_\mu(0)\|\boldsymbol{c}$. This implies that the real $\theta_M^{\perp c\|c}$ should be ~74° and is almost equivalent to $\theta_M^{\perp c\perp c}$ as expected. The A_M signal is therefore found to be caused by $\boldsymbol{H}_{int}$ parallel to the c axis within $\sim\pm15°$. This is very consistent with the anisotropic $\chi(T)$ curve [see Fig. 6(c)], which suggests FM order predominantly along the c axis. Since the monoclinic distortion of Pb_x–BSCO is rather small, i.e., the angle between a and c axis (β_m) ranges between 3.6° and 2.3° for the samples with $x\leq0.4$,[9] the anisotropic μ^+SR result is likely to show a small canting of the FM moments from the c axis.

For the related compound Na_xCoO_2 (NCO), the A-type AF order, in which Co moments align ferromagnetically along the c axis in the CoO_2 plane but antiferromagnetically between the two adjacent CoO_2 planes, was detected for NCO with $x=0.75$ and 0.82 by neutron-diffraction

measurements.[19,20] The appearance of FM order in the CoO_2 plane is therefore reasonable for $Pb_{0.4}$−BSCO. The lack of *A*-type AF order is most likely due to the following three reasons: that is, the absence of magnetic ions in the $[Bi_{2-x}Pb_xSr_2O_4]$ block, the larger distance between the adjacent CoO_2 planes for Pb_x−BSCO than that for NCO, and the misfit between the $[Bi_{2-x}Pb_xSr_2O_4]$ block and the CoO_2 plane. These naturally suppress or eventually annihilate the interplane interaction of Pb_x−BSCO, leading to two-dimensional-FM order in the CoO_2 plane and the absence of three-dimensional-AF order even at 1.8 K for $Pb_{0.4}$−BSCO.

B. Wide field distribution

Figure 6(b) indicates that majority of μ^+'s are likely to stop only at one site because $N_{A_M} \geq 0.9$ at 1.8 K. For the related compound $Na_{0.5}CoO_2$, although the electrostatic potential calculation suggests that the μ^+'s are most likely to sit only at one site, i.e., ~1 Å away from the O ions in the CoO_2 plane,[21] several frequencies were clearly observed below T_N.[10,15,21–24] This has been qualitatively explained by considering both the small deviation of Na positions and the occupancy/vacancy of the Na sites. Unfortunately, because of the misfit between the $[Bi_{2-x}Pb_xSr_2O_4]$ block and the CoO_2 plane along the *b* direction, it is very difficult to calculate the stable μ^+'s sites for Pb_x−BSCO. However, since f_M for $Pb_{0.4}$−BSCO is comparable to those for NCO and K_xCoO_2.[10,15,21–24] We assume that μ^+'s also sit at the vicinity of the O ions in the CoO_2 plane for Pb_x−BSCO. The misfit then naturally produces a spatial modulation of the stable μ^+'s site along the *b* axis. In other words, the position of the μ^+'s changes slightly along the *b* axis, periodically, but incommensurate to the period of the CoO_2 plane. This means that each μ^+ feels a slightly different $\boldsymbol{H}_{\rm int}$ depending on its position. As a result, although there would be several distinct frequencies below T_M as in the case for NCO, those frequencies are most likely to merge into one f_M with a wide distribution. This is the acceptable reason for the KT-type damped cosine oscillation in the ZF spectrum for Pb_x−BSCO [see Figs. 4, 5, and 8(a)]. We wish to emphasize that one can only draw reliable conclusions through the magnetic isotropy/anisotropy by studying single crystals and not powders.

V. SUMMARY

In order to clarify the existence/absence of magnetic order, which is thought to be related to a metal-to-insulator transition around 60 K seen in the temperature dependence of resistivity, the microscopic magnetic nature of pure and Pb-doped $Bi_2Sr_2Co_2O_y$ crystals was investigated by positive muon-spin rotation and relaxation (μ^+SR) spectroscopy in the temperature range between 1.8 and 200 K. ZF-μ^+SR measurements clearly demonstrate that the sample is entirely paramagnetic above 1 K for the pure crystal (above 5 K for the Pb-doped crystal), confirming the absence of static magnetic order. However, since wLF measurements show an increase in the magnetic inhomogeneity below around 60 K for both crystals, a small change in the magnetic nature is found to occur at 60 K, which is naturally considered to correlate with their transport anomaly.

ACKNOWLEDGMENTS

This work was performed both at the TRIUMF, Canada's National Laboratory for Particle and Nuclear Physics in Vancouver (Canada) and at the Swiss Muon Source, Paul Scherrer Institut in Villigen (Switzerland). We thank the staff of both facilities for their help with the μ^+SR experiments. Y.I. and J.S. are partially supported by the KEK-MSL Inter-University Program for Oversea Muon Facilities and J.H.B. is supported at UBC by CIfAR, NSERC of Canada, and (through TRIUMF) by NRC of Canada. K.H.C. is supported by NSERC of Canada and (through TRIUMF) by NRC of Canada. This work is also supported by Grant-in-Aid for Scientific Research (B) with Grant No. 19340107 by MEXT of Japan.

*e0589@mosk.tytlabs.co.jp

[1] A. C. Masset, C. Michel, A. Maignan, M. Hervieu, O. Toulemonde, F. Studer, B. Raveau, and J. Hejtmanek, Phys. Rev. B **62**, 166 (2000).
[2] Y. Miyazaki, K. Kudo, M. Akoshima, Y. Ono, Y. Koike, and T. Kajitani, Jpn. J. Appl. Phys., Part 2 **39**, L531 (2000).
[3] Y. Miyazaki, T. Miura, Y. Ono, and T. Kajitani, Jpn. J. Appl. Phys., Part 2 **41**, L849 (2002).
[4] M. Hervieu, A. Maignan, C. Michel, V. Hardy, N. Creon, and B. Raveau, Phys. Rev. B **67**, 045112 (2003).
[5] J. Sugiyama, H. Itahara, T. Tani, J. H. Brewer, and E. J. Ansaldo, Phys. Rev. B **66**, 134413 (2002).
[6] J. Sugiyama, J. H. Brewer, E. J. Ansaldo, H. Itahara, K. Dohmae, Y. Seno, C. Xia, and T. Tani, Phys. Rev. B **68**, 134423 (2003).
[7] J. Sugiyama, J. H. Brewer, E. J. Ansaldo, H. Itahara, K. Dohmae, C. Xia, Y. Seno, B. Hitti, and T. Tani, J. Phys.: Condens. Matter **15**, 8619 (2003).
[8] T. Yamamoto, K. Uchinokura, and I. Tsukada, Phys. Rev. B **65**, 184434 (2002).
[9] T. Fujii, I. Terasaki, T. Watanabe, and A. Matsuda, Jpn. J. Appl. Phys., Part 2 **41**, L783 (2002).
[10] J. Sugiyama, J. H. Brewer, E. J. Ansaldo, H. Itahara, T. Tani, M. Mikami, Y. Mori, T. Sasaki, S. Hébert, and A. Maignan, Phys. Rev. Lett. **92**, 017602 (2004).
[11] I. Tsukada, T. Yamamoto, M. Takagi, T. Tsubone, S. Konno, and K. Uchinokura, J. Phys. Soc. Jpn. **70**, 834 (2001).
[12] M. L. Foo, Y. Wang, S. Watauchi, H. W. Zandbergen, T. He, R. J. Cava, and N. P. Ong, Phys. Rev. Lett. **92**, 247001 (2004).
[13] G. M. Kalvius, D. R. Noakes, and O. Hartmann, in *Handbook on the Physics and Chemistry of Rare Earths*, edited by K. A. Gschneidner, Jr., L. Eyring, and G. H. Lander (Elseiver, Amsterdam, 2001), Vol. 32, Chap. 206.
[14] G. Solt, Hyperfine Interact. **96**, 167 (1995).
[15] P. Mendels, D. Bono, J. Bobroff, G. Collin, D. Colson, N. Blan-

chard, H. Alloul, I. Mukhamedshin, F. Bert, A. Amato, and A. D. Hillier, Phys. Rev. Lett. **94**, 136403 (2005).
[16] P. J. Baker, T. Lancaster, S. J. Blundell, M. L. Brooks, W. Hayes, D. Prabhakaran, and F. L. Pratt, Phys. Rev. B **72**, 104414 (2005).
[17] L. E. Wenger and P. H. Keesom, Phys. Rev. B **11**, 3497 (1975).
[18] J. Bobroff, S. Hébert, G. Lang, P. Mendels, D. Pelloquin, and A. Maignan, Phys. Rev. B **76**, 100407(R) (2007).
[19] S. P. Bayrakci, I. Mirebeau, P. Bourges, Y. Sidis, M. Enderle, J. Mesot, D. P. Chen, C. T. Lin, and B. Keimer, Phys. Rev. Lett. **94**, 157205 (2005).
[20] L. M. Helme, A. T. Boothroyd, R. Coldea, D. Prabhakaran, D. A. Tennant, A. Hiess, and J. Kulda, Phys. Rev. Lett. **94**, 157206 (2005).
[21] J. Sugiyama, Y. Ikedo, P. L. Russo, H. Nozaki, K. Mukai, D. Andreica, A. Amato, M. Blangero, and C. Delmas, Phys. Rev. B **76**, 104412 (2007).
[22] J. Sugiyama, H. Nozaki, Y. Ikedo, K. Mukai, J. H. Brewer, E. J. Ansaldo, G. D. Morris, D. Andreica, A. Amato, T. Fujii, and A. Asamitsu, Phys. Rev. Lett. **96**, 037206 (2006).
[23] J. Sugiyama, H. Itahara, J. H. Brewer, E. J. Ansaldo, T. Motohashi, M. Karppinen, and H. Yamauchi, Phys. Rev. B **67**, 214420 (2003).
[24] J. Sugiyama, Y. Ikedo, P. L. Russo, K. Mukai, H. Nozaki, J. H. Brewer, E. J. Ansaldo, K. H. Chow, D. Andreica, A. Amato, T. Fujii, A. Asamitsu, K. Ariyoshi, and T. Ohzuku, J. Mater. Sci.: Mater. Electron. **19**, 883 (2008).